





Article

Measurement of Ultra-High Speed by Optical Multistage Cascade Frequency Reduction Technology

Heli Ma ¹, Long Chen ¹ , Wei Gu ¹, Cangli Liu ¹, Longhuang Tang ¹ , Xing Jia ¹, Tianjiong Tao ¹, Shenggang Liu ¹, Yongchao Chen ¹ , Xiang Wang ¹, Jian Wu ¹, Chengjun Li ¹, Dameng Liu ², Jidong Weng ^{1,*} and Huan Liu ^{2,*} 

¹ National Key Laboratory of Shock Wave and Detonation Physics, Institute of Fluid Physics, China Academy of Engineering Physics, Mianyang 621900, China; marcos12@126.com (H.M.); chenlongcaep@163.com (L.C.); 17388398976@163.com (W.G.); cangliliu@aliyun.com (C.L.); tanglonghuang@tju.edu.cn (L.T.); jiaxing@caep.cn (X.J.); zjuttj@163.com (T.T.); liushenggangpla@126.com (S.L.); ychen16@fudan.edu.cn (Y.C.); xiangwang102@126.com (X.W.); ceuwj@zju.edu.cn (J.W.); lstrus@126.com (C.L.)

² State Key Laboratory of Tribology in Advanced Equipment, Department of Mechanical Engineering, Tsinghua University, Beijing 100084, China; ldm@tsinghua.edu.cn

* Correspondence: wengjd1234@126.com (J.W.); liuhuanskt@163.com (H.L.)

Abstract: In order to reduce the frequency of high-frequency Doppler signal light, the electronic bandwidth of a data acquisition system is reduced. This paper mainly describes the principle and experimental verification results of optical multistage cascade frequency reduction technology. The bandwidth requirement of the detector and the oscilloscope is reduced by the method of “relaying” the measured beat frequency signal between multiple electronic channels. Aiming to achieve the requirement of ultra-high speed measurement of 22 km/s, the requirement of the original signal frequency as high as 28 GHz electrical bandwidth is reduced to the acquisition and recording system with only 8 GHz bandwidth. A complete velocity profile of up to 11.47 km/s is measured on a three-stage light gas gun with velocity measurement accuracy of 1%.

Keywords: shock loading; ultra-high speed; laser interferometer; frequency reduction



Citation: Ma, H.; Chen, L.; Gu, W.; Liu, C.; Tang, L.; Jia, X.; Tao, T.; Liu, S.; Chen, Y.; Wang, X.; et al. Measurement of Ultra-High Speed by Optical Multistage Cascade Frequency Reduction Technology. *Appl. Sci.* **2024**, *14*, 10771. <https://doi.org/10.3390/app142310771>

Academic Editor: Andreas Fischer

Received: 9 October 2024

Revised: 13 November 2024

Accepted: 14 November 2024

Published: 21 November 2024



Copyright: © 2024 by the authors. Licensee MDPI, Basel, Switzerland. This article is an open access article distributed under the terms and conditions of the Creative Commons Attribution (CC BY) license (<https://creativecommons.org/licenses/by/4.0/>).

1. Introduction

The use of a Displacement Interferometer System for Any Reflector (DISAR) has become one of the standard techniques for velocity measurement in shock wave and detonation physics experiments [1]. A DISAR with an all-fiber structure gives full play to its characteristics of strong reliability, simple operation and maintenance, and flexible arrangement of measuring points [2]. It has been successfully applied to various high-pressure loading experiments such as those using two-stage light gas guns, high-energy lasers, explosive detonation, pulse power drive, etc. [3–5]. It has become the first choice for measuring material velocity profiles under extreme strain rate loading at present. However, its technical route determines that the system needs fairly high electronic bandwidth, especially when the speed exceeds 10 km/s, wherein the bandwidth needs to be more than 13 GHz [6–8].

At the beginning of the establishment of Photonic Doppler Velocimetry (PDV), researchers at home and abroad noticed the cost increase for recording equipment caused by the increase in the upper limit of speed measurement [9–11]. Therefore, various speed measurement methods of “optical down-conversion” were put forward; that is, by interfering with intrinsic light with frequency shifts and signal light carrying Doppler information, the frequency change of interfering light produced a “mirror image folding in half” with time and was captured by recording equipment [12]. At present, this kind of “optical down-conversion” is a common method when measuring at ultra-high speeds above 20 km/s, but the recording equipment still needs to have a bandwidth of at least 13 GHz [13]. J. G. Mance of NNSC and others proposed “Time-Stretched Photonic Doppler Velocimetry (TS-PDV)”

based on the large dispersion effect of kilometer-long fibers, so as to further reduce the frequency of interference light. Although TS-PDV technology can considerably reduce the pressure on the bandwidth of recording equipment during ultra-high-speed measurement, there are still numerous uncontrollable experimental parameters, so it has remained in the verification stage, but it is still worthy of follow-up as a research direction [14,15].

Based on the principle of optical heterodyne Doppler velocimetry, this paper presents multi-stage cascade velocimetry technology which can considerably reduce the frequency of ultra-high-speed Doppler signals. In this paper, the method of frequency reduction technology and multi-level signal splicing using down-conversion signals is proposed to realize high-speed signal frequency reduction. It breaks through the limitation of bandwidth to the upper limit of velocity measurement and realizes the continuous measurement of ultra-high-speed (22 km/s) motion profiles with an oscilloscope (bandwidth of 8 GHz).

2. Principle

2.1. Light Path Construction

In most cases, a DISAR illuminates a moving target with light with wavelength λ_1 (velocity u), collects reflected Doppler signal light λ_1' , and mixes the signal light with reference light λ_2 . Therefore, the mixed beat frequency signal is as follows:

$$v_B = \left| \frac{c}{\lambda_1'} - \frac{c}{\lambda_2} \right| \approx \left| \frac{c}{\lambda_1} - \frac{c}{\lambda_2} + \frac{2u}{\lambda_1} \right| \quad (1)$$

The size of the beat frequency signal is determined by the speed u of the target motion and the wavelength of the reference light. Normally, the beat optical signal is converted into an electrical signal by a rapid photodetector and recorded by a digital oscilloscope. In most devices, $\lambda_1 = \lambda_2$ is commonly set, which is DISAR or PDV technology.

Because a DISAR generally uses a laser with a wavelength of 1550 nm, every 1 km/s speed requires an electronic bandwidth of about 1.3 GHz. It is unrealistic to track a moving target as high as 20 km/s using only a single-channel DISAR. A beat frequency signal is divided into multiple channels to reduce the bandwidth requirement of the detector and oscilloscope, so that the measured beat frequency signal can be “relayed” among multiple electronic channels. This technology can be called multi-stage cascade technology.

Taking the two-stage cascade technology as an example, as shown in Figure 1, the main laser (wavelength: 1550.256 nm; power: 1 W) emits continuous single-frequency laser to the optical fiber probe through the second port of the optical fiber circulator, and the probe irradiates the measured surface and receives the reflected signal light, which is a heterodyne with reference laser 1 (wavelength: 1550.128 nm; power: 50 mW) and reference laser 2 (wavelength: 1550.000 nm; power: 50 mW).

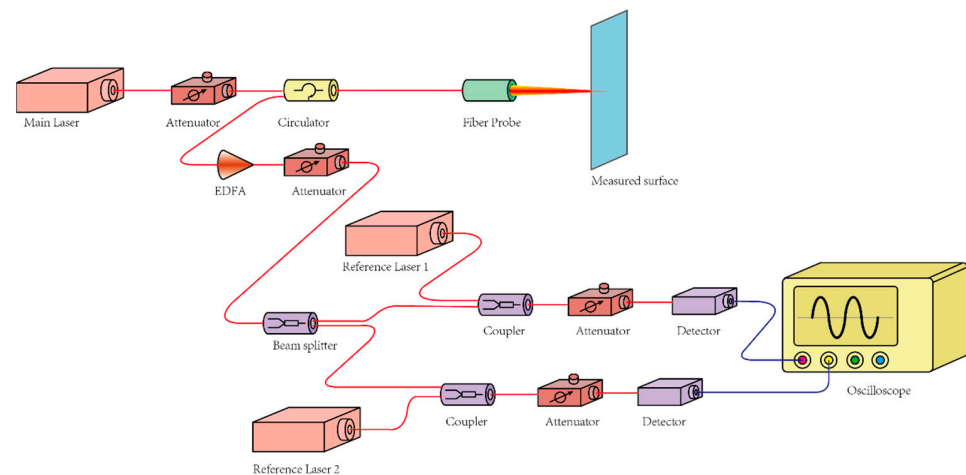


Figure 1. Schematic diagram of optical cascade frequency reduction optical path.

Assuming that the wavelengths of the main laser, reference laser 1, and reference laser 2 are λ_1 , λ_2 , and λ_3 , respectively, and the velocity of the target to be measured is u , then the velocity u_1 obtained by channel 1 after the first frequency reduction and the velocity u_2 obtained by channel 2 after the second frequency reduction are, respectively, as follows:

$$u_1 = \frac{\lambda_1}{2} \left| f_d - \left(\frac{c}{\lambda_2} - \frac{c}{\lambda_1} \right) \right| \tag{2}$$

$$u_2 = \frac{\lambda_1}{2} \left| f_d - \left(\frac{c}{\lambda_3} - \frac{c}{\lambda_1} \right) \right| \tag{3}$$

where f_d is Doppler shift.

If the speed signal is a straight line motion with uniform acceleration, that is, a straight line signal with a fixed slope, as shown in Figure 2a, then Equations (2) and (3) correspond to the green and blue curves in Figure 2b, respectively. Due to the limitation of the bandwidth f_{BW} of the acquisition system, the actual channel 1 and channel 2 can only record the signals in the green and blue boxes, respectively. The final complete speed curve can be “restored” by “flipping” the two signals and “splicing” the end and end. This is the frequency reduction effect that can be achieved by a two-stage cascade. By selecting the appropriate reference laser wavelength, the recording system that originally needed quadruple bandwidth can be reduced to only one bandwidth.

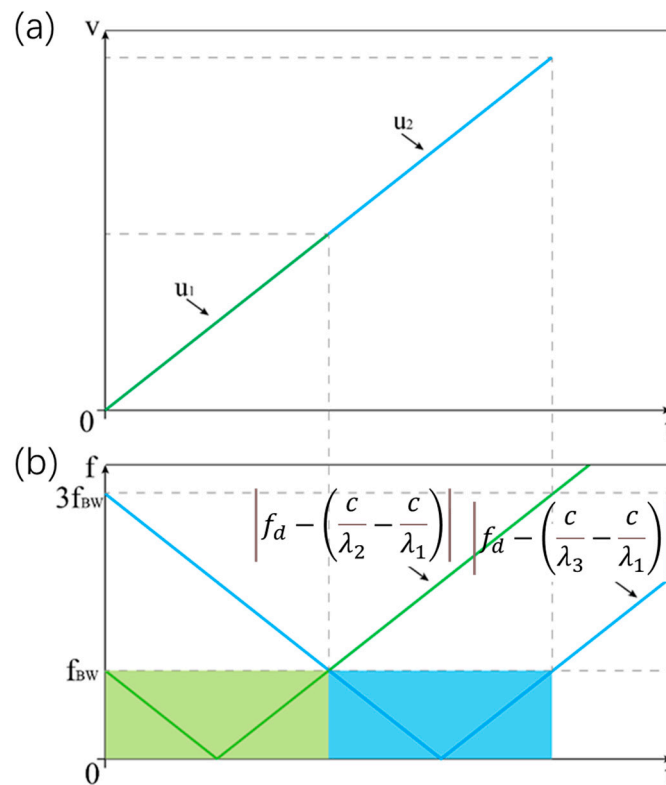


Figure 2. Schematic diagram of the corresponding relationship between (a) velocity curve and (b) two-stage cascade frequency signal.

Each stage of frequency reduction can reduce the signal frequency by half, so when N-stage cascade frequency reduction technology is adopted, the original signal frequency can be reduced by $2N$ times, and there is no upper limit on the frequency reduction multiple of signal frequency in theory. However, it is worth noting that every time the frequency reduction is added, the original signal needs to be divided into one part for an optical heterodyne. When the frequency reduction is made by N stages, the signal strength of each stage is only $1/N$ of the original signal strength, so it is necessary to amplify the signal

first. At the same time, in order to improve the contrast and signal-to-noise ratio of the interference signal, it is necessary to attenuate the power and adjust the balance of signal light and reference light, respectively. If the signal-to-noise ratio decreases due to increased noise, the contrast between the frequency curve and the background in the spectrogram decreases. This will lead to an increase in the error of the proposed speed signal frequency and an increase in the error when the two signals are spliced.

2.2. Simulation Verification

Using OptiSystem 15.0 software, the optical path shown in Figure 2 is designed and optimized in further detail. The optical path structure is established in the software. The optical path is the same as the two-stage optical cascade frequency reduction optical path introduced in the principle analysis, and it is designed based on the premise that the data acquisition system (oscilloscope) has 8 GHz bandwidth frequency response. According to the principle of two-stage optical cascade frequency reduction analyzed above, the central wavelengths of three lasers are set at intervals with the bandwidth of data recording system as the scale, and the linewidth and power of lasers are defined, as shown in Table 1.

Table 1. Parameter setting of each laser in simulation.

Name	Wavelength/nm	Line Width/kHz	Power/mW	Relative Intensity Noise/dB/Hz
Main Laser	1550.192	100	500	−130
Reference Laser 1	1550.128	100	50	−130
Reference Laser 2	1550.000	100	50	−130

In the simulation, the circulator isolation has a great influence on the interference signal quality, so it is focused on its evaluation. Because the isolation between ports 1 and 3 of the circulator is not ideal (infinite), a limited amount of light energy output by the main laser will directly leak into the photodetector through the path of ports 1–3. The beam light and the signal light will be mixed to generate an additional “ghosting” signal, which will affect the extraction of spectral features. Under the current process conditions, the typical isolation between ports 1 and 3 of the circulator is 55–60 dB. When 55 dB is selected as the measured value, the gain of the photoelectric amplification module is controlled in the range of 15–30 dB (with 10 gain points taken at equal intervals), and the leakage optical power curve input to the photoelectric conversion module is obtained, as shown in Figure 3.

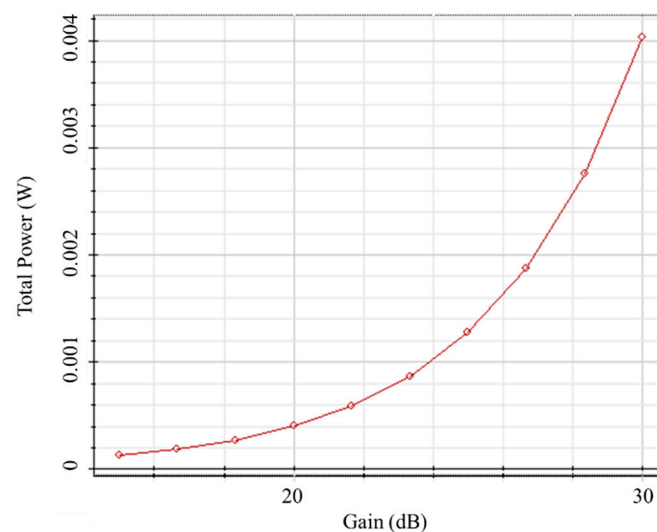


Figure 3. Leakage optical power input to photoelectric conversion module under different gains.

It can be seen from the simulation results that the maximum leakage optical power is about 360 nW. By setting a virtual RF spectrometer at the back end of the photoelectric conversion module, the signal spectrum generated by mixing leakage light with reference lasers 1 and 2 can be analyzed, and the results are shown in Figure 4. Figure 4a shows the frequency spectrum of the mixed signal generated by the leakage light and the output light of reference laser 1. It can be seen that there is a characteristic peak at 7.96 GHz, which is virtually consistent with the frequency difference (8 GHz) between the two lasers. Figure 4b shows the frequency spectrum of the mixed signal generated by the leakage light and the output light of reference laser 2. It can be seen that there is a characteristic peak at 23.90 GHz, which is approximately consistent with the frequency difference (24 GHz) between the two lasers.

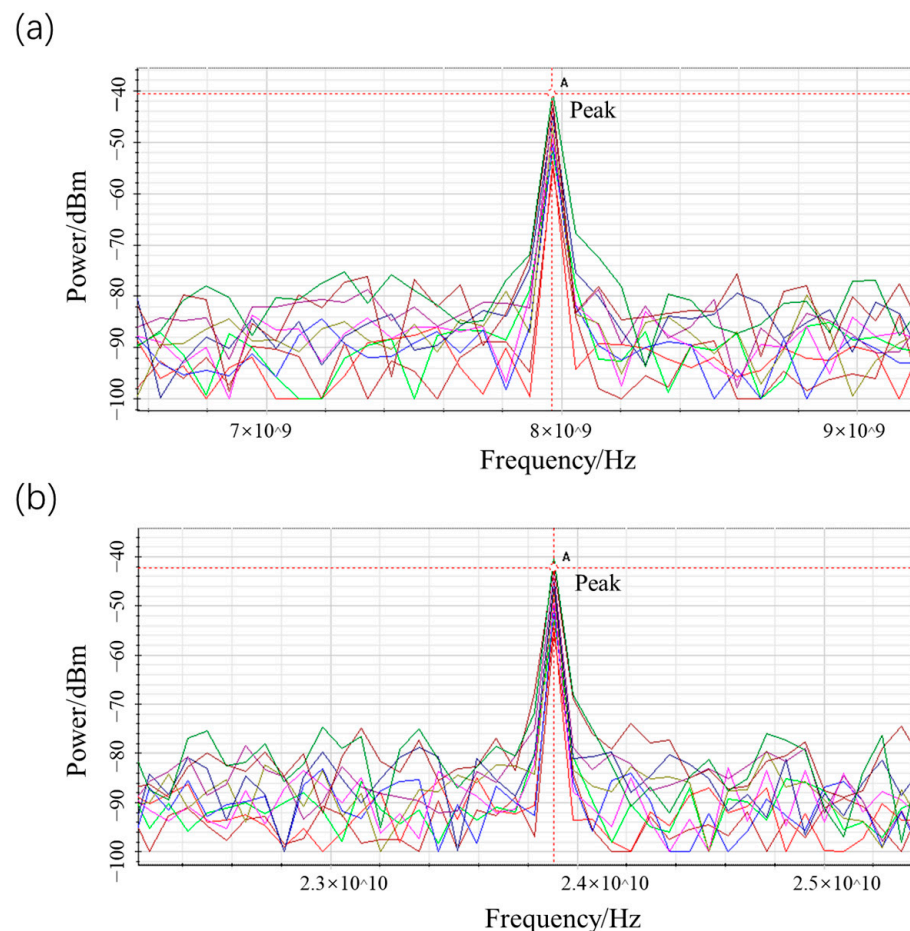


Figure 4. Frequency spectrum of mixed signal generated by leakage light and output light of (a) reference laser 1 and (b) reference laser 2.

In order to additionally evaluate the quality of interference signal, a tuned laser is set at the probe end of the optical path, and the frequency change of its output light (signal light) simulates the Doppler frequency shift caused by the velocity change in the measured target. In the simulation, the tuning laser power is set to 50 μ W, and the frequency sweeps 10 points in turn. Through the virtual oscilloscope set at the back end of the photodetector, the virtual interference signal can be obtained by simulation.

3. Discussion and Results

3.1. Simulation

Virtual oscilloscopes 1 and 2 record signals generated by mixing signal light with reference lasers 1 and 2, respectively. Figure 5 shows the signals captured in two virtual

oscilloscopes when the tuned laser wavelength is 1550.192 nm. Clear interference fringe signals can be seen from the virtual oscilloscope, in which the period of the signal in the first oscilloscope is 0.129 ns, and the corresponding signal frequency is 7.74 GHz, which is -0.06 GHz different from the design value of 8 GHz, as shown in Figure 5a. The period of the signal in the second oscilloscope is 0.046 ns, and the corresponding signal frequency is 21.7 GHz, which is -2.3 GHz different from the design value of 24 GHz, as shown in Figure 5b.

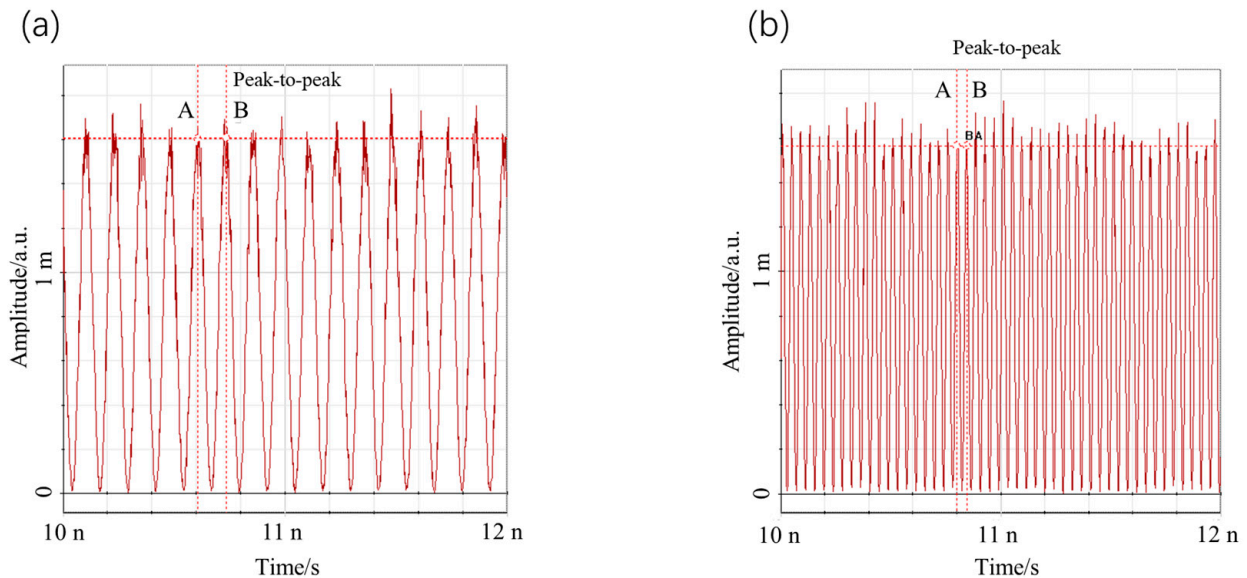


Figure 5. Interference signals in (a) virtual oscilloscope 1 and (b) virtual oscilloscope 2.

Through the virtual radio frequency spectrometer set at the back end of the photoelectric conversion module, the spectrum of interference signals can be further analyzed. Virtual RF spectrometers 1 and 2, respectively, record the frequency spectrum of the signal generated by mixing the signal light with tunable lasers 1 and 2, which correspond to the first-stage frequency conversion spectrum and the second-stage frequency conversion spectrum, respectively. Figure 6a,b show the first-stage frequency conversion spectrum recorded by virtual RF spectrometer 1 when the tuned laser wavelengths are 1550.176 nm and 1550.048 nm, respectively. Three characteristic peaks can be observed in both spectra: (1) The first characteristic peak is located at about 8 GHz (point B in Figure 6a and point C in Figure 6b), which is formed by interference between leakage light and output light of reference laser 1, and its position does not alter during frequency conversion, which is a fundamental frequency signal. (2) The second characteristic peak is formed by interference between the signal light and the output light of reference laser 1, and it corresponds to point A in Figure 6a,b. The peak has higher intensity than other peaks and is a normal signal (frequency conversion signal) that can be expected to be obtained. (3) The third characteristic peak is formed by the interference of signal light and leakage light, corresponding to point C in Figure 6a and point B in Figure 6b, and the position of the peak moves with the shift of light wavelength, which is a ghost signal and is linear.

Figure 6c shows the second-stage frequency conversion spectrum recorded by virtual RF spectrometer 2 when the tuned laser wavelengths are 1550.048 nm, respectively. The spectrum of “three characteristic peaks” is similar to those in Figure 6a,b, in which point A is the characteristic peak of fundamental frequency signal, which is 23.92 GHz; and point B is the characteristic peak of ghost signal, which is 17.97 GHz; and point C is the characteristic peak of frequency conversion signal, which is 5.96 GHz.

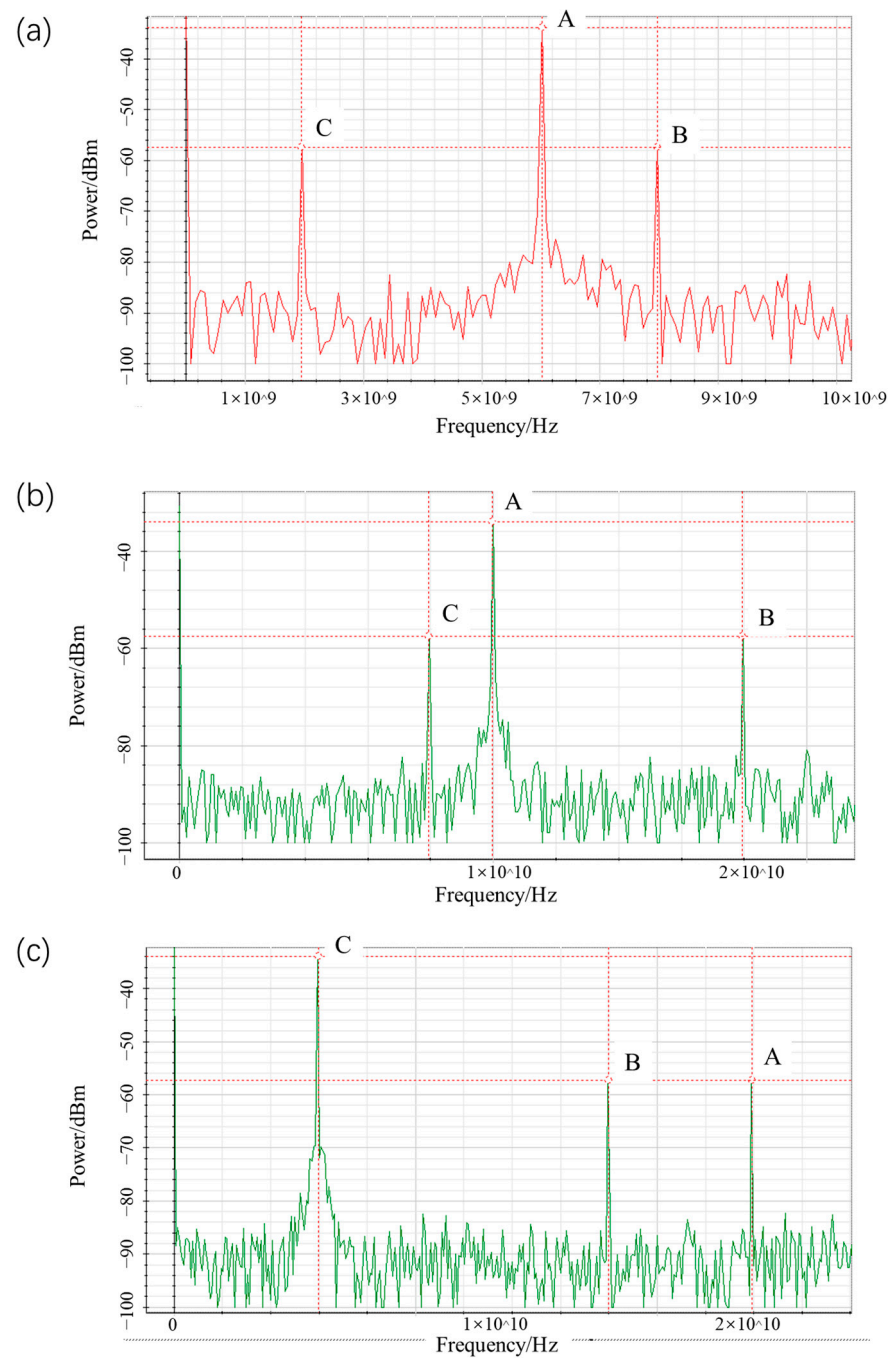


Figure 6. (a) First-stage frequency conversion spectrum (tuned laser wavelength is 1550.176 nm); (b) first-stage frequency conversion spectrum (tuned laser wavelength is 1550.048 nm); (c) frequency spectrum of the second stage (tuned laser wavelength is 1550.048 nm).

By reading the frequency spectrum of each sweep frequency point and drawing the intensity map, the two-dimensional frequency spectrum of the frequency conversion signal can be generated. The wavelength of the tuned laser is 10 points at equal intervals between 1550.256 nm and 1549.936 nm, and the two-dimensional spectrum diagram drawn is shown in Figure 7. Figure 7a is generated by the spectrum collected by virtual RF spectrometer 1, which is the first-stage frequency conversion spectrum. Figure 7b is generated by the spectrum collected by virtual RF spectrometer 2, which is the second-stage frequency conversion spectrum.

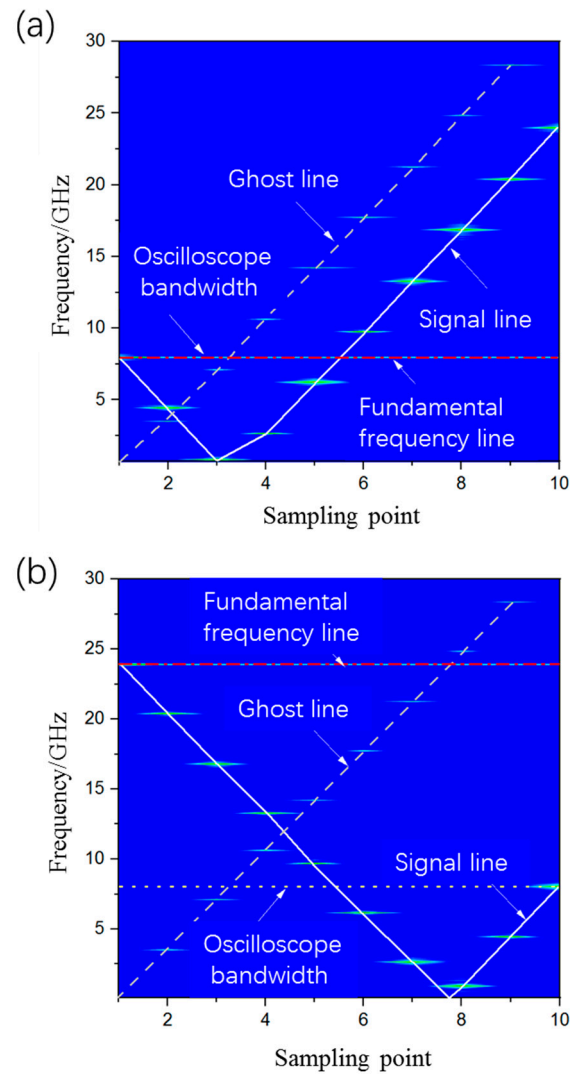


Figure 7. (a) First-stage two-dimensional frequency conversion spectrum; (b) two-dimensional frequency conversion spectrum of the second stage.

From Figure 7, the evolution characteristics of the three types of signals can be analyzed. Among them, the fundamental frequency line generated by the shift in the fundamental frequency signal with the sweep frequency point has obvious broken line characteristics. Ghost signals are characterized by linear changes, which will overlap across signal lines. The fundamental frequency line does not move with the shift in the sweep frequency point, but it also crosses the signal line. In the first-stage frequency conversion spectrum, it can be seen that the overlap between the ghost line and the fundamental frequency line and the signal line occurs in the area covered by the oscilloscope bandwidth (8 GHz), which can be recorded by an oscilloscope, so it has an impact on the actual signal line extraction. However, it can be seen from the second-stage frequency conversion spectrum that the overlap of the hatching line, fundamental frequency line, and signal line occurs outside the area covered by the oscilloscope bandwidth (8 GHz), which will not affect the extraction of the actual speed line, but the trend of the ghosting line is similar to that of the signal line after turning.

3.2. Laser Wavelength Tuning Experiment

At present, there is no standard speed source used in the measurement of high-speed test equipment, and a Doppler velocimeter is essentially a frequency meter, so the frequency measurement ability of a velocimeter in a wide speed domain can only

be evaluated by establishing an analog speed signal [16]. The laser wavelength tuning experiment is designed. The laser wavelength is changed by the long thermal tuning function of the resonator and the laser wavelength is interfered with using the reference light inside the velocimeter to form an optical beat signal, which simulates the optical Doppler frequency shift characteristics when the object moves at elevated speed. By examining the frequency response characteristics of the velocimeter under the optical beat signal at different frequency points, the velocity measurement ability of the velocimeter is evaluated.

The output fiber of the tunable laser is directly connected with the optical output port of the velocimeter, and the RF output port of the velocimeter is connected with the spectrum analyzer. The initial wavelength setting of the tunable fiber laser is the same as that of the frequency-stabilized laser module in the velocimeter. By adjusting the wavelength of the tunable fiber laser to different wavelength points and measuring the RF signal frequency of the optical beat after photoelectric conversion with the spectrum analyzer, the speed measurement range can be evaluated. The wavelength tuning range of the tunable fiber laser is 0.1~227.1 pm (corresponding to the frequency of 12.5~28.4 GHz) when the measuring speed range is 10~22 km/s.

The rate of the shift in the optical beat frequency generated by the two-stage optical path with wavelength is obtained, as shown in Figure 8. The optical beat rate of the primary channel is 124.73 GHz/nm and -124.63 GHz/nm, and that of the secondary channel is 126.44 GHz/nm and -126.88 GHz/nm. The optical beat frequency varies linearly with wavelength. In actual measurement, the rate of the shift in two-stage optical beats needs to be calibrated before the experiment, so as to obtain a more accurate velocity profile.

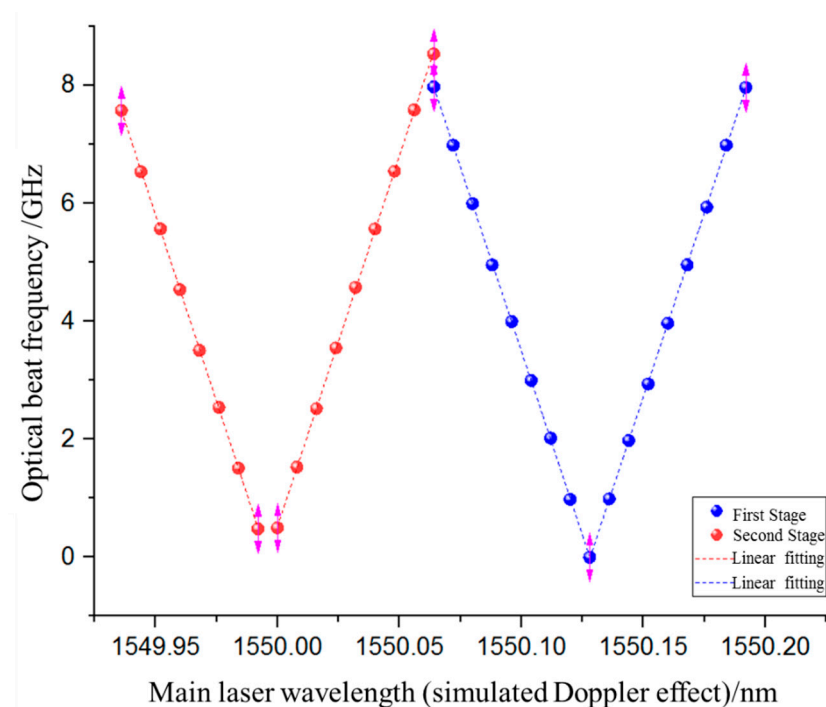


Figure 8. Linear fitting results of optical beat frequency.

This experiment can obviously measure the characteristics of laser frequency shift, which are similar to the characteristics of interface velocity shift in the typical impact loading process. It can verify the principle feasibility of multi-cascade laser interferometric velocimetry technology.

3.3. Impact Loading Experiment of Three-Stage Light Gas Gun

In order to further verify the dynamic test performance of multi-cascade superheterodyne laser interferometry, the impact loading experiment of a three-stage light gas gun was carried out. The principle, device, and experimental site of the three-stage light gas gun are shown in Figure 9. The flyer is composite gradient materials and the target sample is steel. Both of them are 1 mm thick, and the distance between them is 10 mm. The launching technology of the three-stage light gas gun is a high-speed launching technology based on the launching technology of a two-stage light gas gun [17,18], which forms “multi-stage pressurization” by multiple reflections of shock waves between different materials in projectile and pushes the speed of target materials to more than 10 km/s. At the back end of the target material, an optical fiber velocimeter probe is installed to transmit and receive optical signals emitted by the velocimeter and reflected by the target material. The DPS probe is a probe with a return loss of 17 dB and is used for zero-differential velocimetry (DPS). The two-stage probe is a probe with a return loss of 60 dB, which is used in this paper for cascaded frequency reduction technology. The trigger probe is a full-return fiber optic probe that uses the change in light intensity to provide an external trigger signal after being impacted.

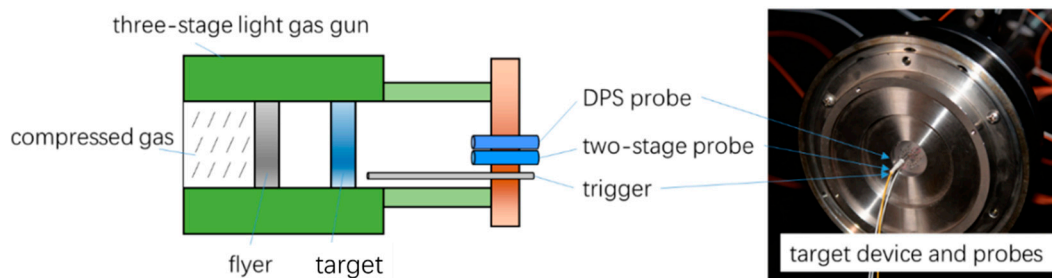


Figure 9. Experimental principle and device of three-stage light gas gun.

In the test, a 5-GHz bandwidth oscilloscope is used as the signal recording equipment. In order to match the oscilloscope bandwidth, the wavelengths of the main laser module and the reference laser module are adjusted to 1550.120 nm, 1550.080 nm, and 1550.000 nm, respectively, and the frequency intervals are 5 GHz and 10 GHz in turn. In this way, the velocity measurement bandwidth of the velocimeter system reaches 20 GHz, and the corresponding maximum measured speed is 15.5 km/s. In order to verify the validity of the measured data of the velocimeter system, synchronous measurement is carried out by using the conventional non-frequency conversion velocimeter system (DPS) [19].

The spectrograms for the conventional DPS (Doppler Pins System) speeds and the two-stage downscaling speeds are shown in Figure 10. According to the principle of laser interferometric velocimetry, that is, $u = 1/2 \cdot \lambda f$, the Doppler frequency f is obtained by using the short-time Fourier transform (STFT) from the interferometric signal, and the impact velocity is obtained by multiplying it with half the wavelength. Through data processing, a relatively complete velocity profile of the target material can be obtained, as shown in Figure 11. The red line is the velocity profile captured by the first stage of the prototype system, the blue line is the velocity profile captured by the second stage, and the black line is the velocity profile captured by the conventional velocity measurement system. The violet line is the displacement curve obtained by the time integration of the DPS velocity curve. Because two-stage downscaling uses a thermal expanded core probe, there is a test blind area when the measured surface is close to the probe, as shown by the dashed box in Figure 11. The maximum velocity profile of 11.47 km/s is measured by the two systems, the measuring time is about 2 μ s, and the measured displacement of target material is about 7.6 mm (depth of field). The first-stage signal is interrupted at 2.7 μ s after triggering, and the second-stage signal starts at 2 μ s after triggering, with a signal relay zone of 0.7 μ s between the two stages. In data processing, the window length

is 512 samples, the Fourier transform length is 4096 samples with the square window, and the product of velocity accuracy and time accuracy is 97 ns·m/s. When the time accuracy is 25.6 ns, the velocity accuracy is 3.8 m/s, and when the time accuracy is 50 ns, the corresponding velocity accuracy is 1.8 m/s, which meets the technical requirements. The experimental results show that the principle of optical multistage cascade frequency reduction technology is feasible.

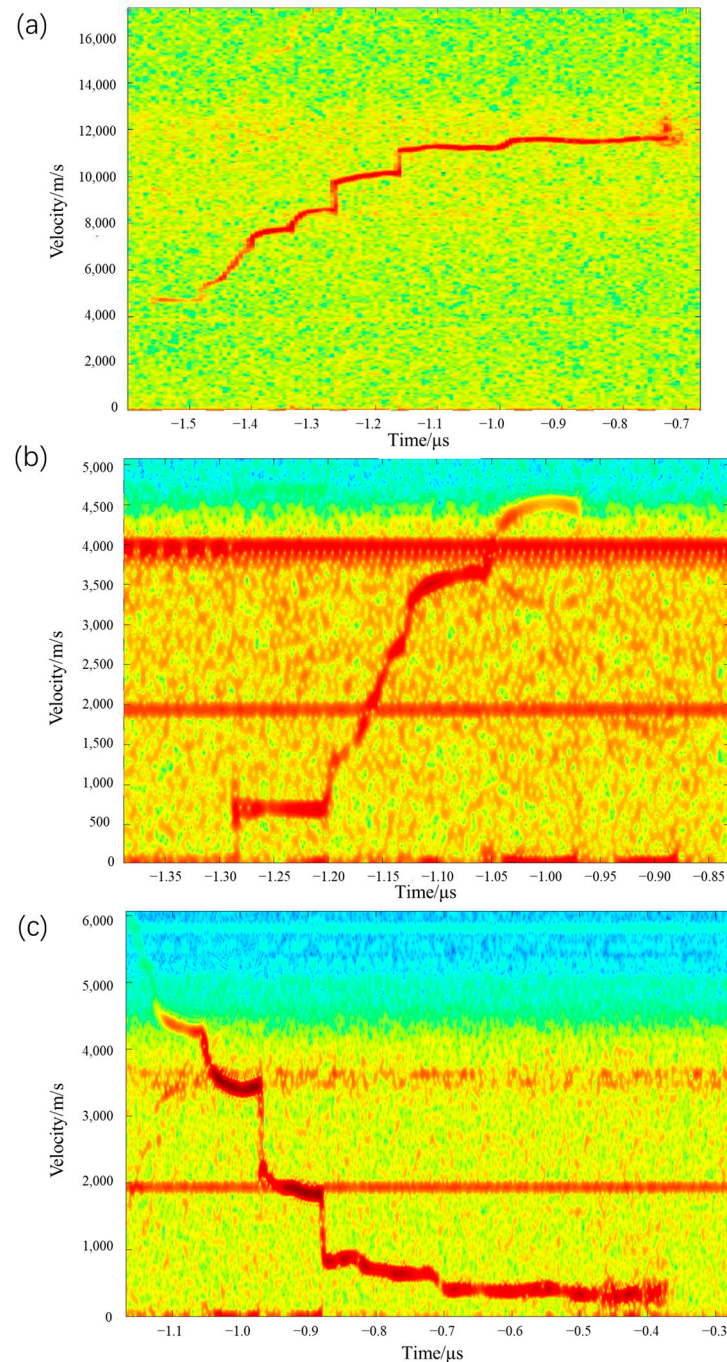


Figure 10. Spectrum diagram of two kinds of velocity measurement results: (a) DISAR, (b) first stage, and (c) second stage.

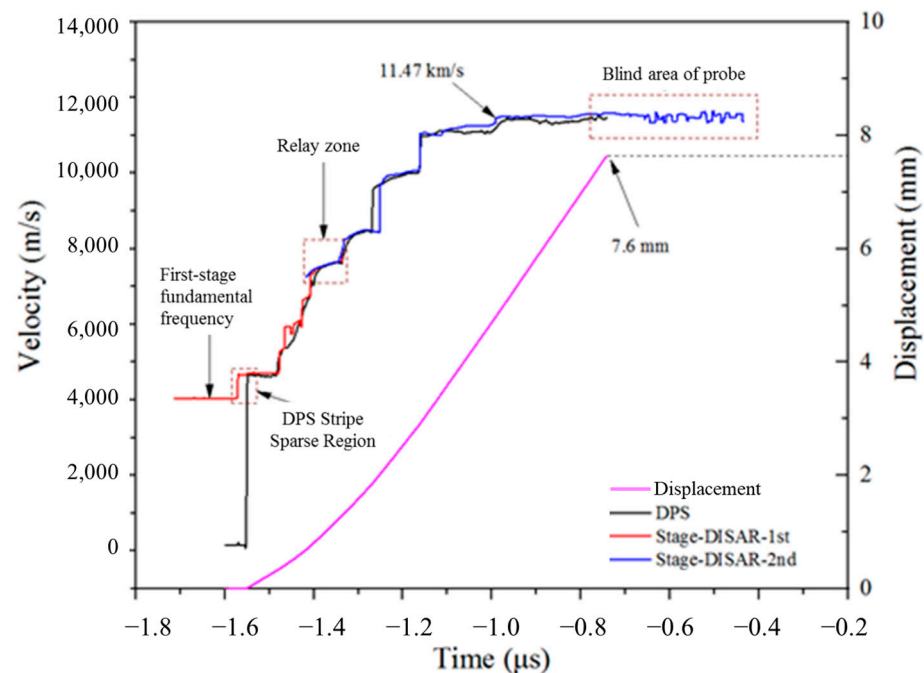


Figure 11. Velocity profiles obtained from experiments.

4. Conclusions

Through two-stage optical cascade frequency reduction, speed segmented “relay” measurement is formed between adjacent stages, and the speed measurement bandwidth has been expanded. If we cascade multi-stage frequency reduction optical paths according to this rule, each multi-stage optical path will increase the speed measurement bandwidth of the system, so the multi-stage cascade frequency reduction technology can theoretically expand the upper limit of speed measurement infinitely.

With multi-stage cascade frequency reduction, the limited-bandwidth digital oscilloscope can be used to achieve the purpose of expanding the bandwidth of multi-time velocity measurement and finally realize ultra-high-velocity profile measurement. The research results of this paper can provide laser interference ultra-high velocity measurement technology with a maximum velocity measurement upper limit of 22 km/s, time resolution of 200 ps, and velocity measurement accuracy of 1%. In the research fields of aerospace industry and natural science, the velocity of objects above 10 km/s or even 20 km/s can be continuously measured in a non-contact way.

Each use of N-cascade downscaling technology can reduce the original signal frequency to $1/N$ of the original signal. For ultra-high-speed signal measurements, the bandwidth requirement of the oscilloscope is reduced by a factor of N , which greatly reduces the cost in engineering applications.

Author Contributions: Conceptualization, J.W. (Jidong Weng); methodology, T.T.; software, Y.C.; and C.L. (Chengjun Li); validation, D.L.; formal analysis, X.J.; investigation, L.T.; resources, S.L.; data curation, W.G.; writing—original draft preparation, L.C.; writing—review and editing, H.M.; visualization, J.W. (Jian Wu); supervision, X.W.; project administration, H.L.; funding acquisition, C.L. (Cangli Liu). All authors have read and agreed to the published version of the manuscript.

Funding: This research was funded by the National Natural Science Foundation of China, grant numbers 62101518, 52105195, and U2241276, and the Foundation of National Key Laboratory of Shock Wave and Detonation Physics, grant number JCKYS2022212001.

Acknowledgments: This work is supported by the China Academy of Engineering Physics.

Conflicts of Interest: The authors declare no conflict of interest.

References

1. Weng, J.; Tan, H.; Wang, X.; Ma, Y.; Hu, S.; Wang, X. Optical-fiber interferometer for velocity measurements with picosecond resolution. *Appl. Phys. Lett.* **2006**, *89*, 111101. [[CrossRef](#)]
2. Weng, J.; Wang, X.; Ma, Y.; Tan, H.; Cai, L.; Li, J.; Liu, C. A compact all-fiber displacement interferometer for measuring the foil velocity driven by laser. *Rev. Sci. Instrum.* **2008**, *79*, 113101. [[CrossRef](#)] [[PubMed](#)]
3. Li, X.M.; Yu, Y.Y.; Li, Y.H.; Zhang, L.; Weng, J.D. Window Corrections of Z-cut Quartz at 1550 Nm Under Elastic, Uniaxial Compression up to 10 GPa. *J. Appl. Phys.* **2011**, *109*, 103518. [[CrossRef](#)]
4. Zhang, H.; Zhao, X.W.; Tan, Y.; He, R.Z.; Huang, J.; Ma, Y.C.; Li, J.; Weng, J.D.; Jin, K. Single femtosecond laser beam pumped transient diffraction and transient lens effects for ultrafast measurement in background-free geometry. *Opt. Laser. Technol.* **2017**, *92*, 189–192. [[CrossRef](#)]
5. Khaustov, S.V.; Pai, V.V.; Lukyanov, Y.L.; Lysak, V.I.; Kuz'min, S.V. Thermal effect of explosive detonation products on a flyer plate in the explosive welding of metals. *Int. J. Heat. Mass. Tran.* **2020**, *163*, 120469. [[CrossRef](#)]
6. Dolan, D.H. Extreme measurements with Photonic Doppler Velocimetry (PDV). *Rev. Sci. Instrum.* **2020**, *91*, 051501. [[CrossRef](#)] [[PubMed](#)]
7. Mercurio, S.; Grace, D.; Bless, S.; Iskander, M.; Omidvar, M. Frequency-shifted photonic Doppler velocimetry (PDV) for measuring deceleration of projectiles in soils. *Acta. Geotech.* **2024**, *19*, 2467–2485. [[CrossRef](#)]
8. Dolan, D.H. Technology and times scales in Photonic Doppler Velocimetry (PDV). *Meas. Sci. Technol.* **2024**, *35*, 061001. [[CrossRef](#)]
9. Jensen, B.J.; Holtkamp, D.B.; Rigg, P.A.; Dolan, D.H. Accuracy limits and window corrections for photon Doppler velocimetry. *J. Appl. Phys.* **2007**, *101*, 013523. [[CrossRef](#)]
10. Gallegos, C.H.; Marshall, B.; Teel, M.; Romero, V.T.; Diaz, A.; Berninger, M. Comparison of Triature Doppler Velocimetry and Visar. *J. Phys. Conf. Ser.* **2010**, *244*, 032045. [[CrossRef](#)]
11. Dolan, D.H.; Lemke, R.W.; McBride, R.D.; Martin, M.R.; Harding, E.; Dalton, D.G.; Blue, B.E.; Walker, S.S. Tracking an imploding cylinder with photonic Doppler velocimetry. *Rev. Sci. Instrum.* **2013**, *84*, 055102. [[CrossRef](#)] [[PubMed](#)]
12. Cavanna, A.; Hammer, J.; Okoth, C.; Ortiz-Ricardo, E.; Cruz-Ramirez, H.; Garay-Palmett, K.; U'Ren, A.B.; Frosz, M.H.; Jiang, X. Progress toward third-order parametric down-conversion in optical fibers. *Phys. Rev. A.* **2020**, *101*, 033840. [[CrossRef](#)]
13. Dolan, D.H.; Ao, T.; Hernandez, O. Note: Frequency-conversion photonic Doppler velocimetry with an inverted circulator. *Rev. Sci. Instrum.* **2012**, *83*, 026109. [[CrossRef](#)] [[PubMed](#)]
14. Mance, J.G.; La Lone, B.M.; Dolan, D.H.; Payne, S.L.; Ramsey, D.L.; Veaser, L.R. Time-stretched photonic Doppler velocimetry. *Opt. Express.* **2019**, *27*, 25022–25030. [[CrossRef](#)] [[PubMed](#)]
15. Kilic, V.; DiMarco, C.S.; Foster, M.A. Time Lens Photon Doppler Velocimetry (TL-PDV) for extreme measurements. *Nat. Commun.* **2024**, *2024*, 1–8. [[CrossRef](#)] [[PubMed](#)]
16. Ambrose, W.P. *Precision and Accuracy in PDV and VISAR*; Lawrence Livermore National Laboratory: San Francisco, CA, USA, 2017; LLNL-TR-737609.
17. Bogdanoff, W.D. Design of a Two-Stage Light Gas Gun for Muzzle Velocities of 10–11 km/s. In Proceedings of the 67th Meeting of the Aeroballistic Range Association, Toledo, Spain, 3–6 October 2016.
18. Thornhill, T.F.; Chhabildas, L.C.; Reinhart, W.D. Particle launch to 19 km/s for micro-meteoroid simulation using enhanced three-stage light gas gun hypervelocity launcher techniques. *Int. J. Impact Eng.* **2006**, *33*, 799–811. [[CrossRef](#)]
19. Fan, Z.N.; Akram, M.S.; Liu, F.S.; Liu, Q.J. Shock temperature of liquid nitrogen under pressure using a combination of multi-channel pyrometer and Doppler pin system. *Phys. Lett. A* **2024**, *519*, 129700.

Disclaimer/Publisher's Note: The statements, opinions and data contained in all publications are solely those of the individual author(s) and contributor(s) and not of MDPI and/or the editor(s). MDPI and/or the editor(s) disclaim responsibility for any injury to people or property resulting from any ideas, methods, instructions or products referred to in the content.